Engineering and Technology Journal e-ISSN: 2456-3358
Volume 11 Issue 02 February-2026, Page No.-8854-8870
DOI: 10.47191/etj/v11i02.09, I.F. – 8.482

Multi-Domain Feature Fusion with OVO-SVM for Multi-Class Motor Imagery EEG Classification and Motor Control Validation

Yahya Ghufran Khidhir[1*], Sarmad Nozad Mahmood[2], Ibrahim AL-Tameemi[3]
[1] Electronic and Control Engineering Techniques Department, Technical Engineering College – Kirkuk, Northern Technical University, Mosul 41001, Iraq
[2] Medical Instrumentation Techniques Engineering Department, Technical Engineering College – Kirkuk, Northern Technical University, Mosul 41001, Iraq
[3] Mechatronics Department, AL-Khwarizmi College of Engineering, University of Baghdad, Baghdad, Iraq

ABSTRACT: The number of people in the world who suffer from a stroke, multiple sclerosis and spinal cord injuries is estimated to reach 2 to 4 percent of the population, often with severe motor disabilities. Electroencephalogram (EEG) based brain-computer interfaces (BCIs) are an effective way of communicating with a person by translating brain signals to meaningful control commands. Motor imagery (MI) based BCIs allow users to control external devices by imagining certain movements. Although conventional methods, such as common spatial pattern (CSP) and power spectral density (PSD), have shown good performance, they may not be able to capture complementary time-frequency and nonlinear characteristics of EEG signals. This study introduces a robust multi-domain framework for four class MI classification using right hand, left hand, foot and tongue imagery. The proposed system uses a combination of CSP, PSD, log variance, wavelet transform and bispectrum analysis to extract the spatial, spectral, temporal and nonlinear features. The one vs. one support vector machine (OVO-SVM) classifier is used to improve the class separability and to address the class imbalance. In addition to classification offline, an end-to-end EEG-driven control architecture is developed, in which decoded motor imagery decisions are directly mapped into coordinated control commands for two independent motors, allowing for continuous translation of cognitive intentions into physical motion. Experimental results show that the performance is good for all subjects, and Subject 3 shows the highest accuracy (95.83%) and Kappa (0.94), while the average accuracy and Kappa are 74.3% and 0.65, respectively. System-Level Validation with Independent Evaluation Dataset Stable temporal prediction behaviour Reliable motor command generation Coordination of multi-motor control Coordination of spatial motion trajectories Stable temporal prediction behaviour Reliable motor command generation Coordination of multi-motor control Coordination of spatial motion trajectories Bridging the Gap between EEG- based Classification and Practical Motor Control Implementation These findings reveal the great potential of the proposed framework for real world MI-based BCI applications.

KEYWORDS: Motor Imagery BCI, EEG Classification, Multi-Domain Features, OVO-SVM, Common Spatial Pattern, Wavelet–Bispectrum, Motor Control Validation.

1. INTRODUCTION

According to estimates by the World Health Organization (WHO), 2-4% of the world population is affected by severe disability or paralysis, a share that is projected to rise with the aging of the population and the rise in chronic disorders, such as stroke, multiple sclerosis and spinal cord injury. In these circumstances, affected individuals can have a complete locked-in syndrome, with a loss of voluntary motor and verbal communication [1]. These deficits reflect the critical importance of Brain- Computer Interfaces (BCIs), high-tech communication tools that create a direct transfer of information between cerebral activity and extraneous devices [2, 3]. A traditional BCI system measures the electrical activity of the brain, extracts salient features, and interprets these features to identify certain mental or cognitive processes [4]. Among the several BCI paradigms, electroencephalography (EEG) based BCIs can be considered the most common, as they are non-invasive, offer better temporal resolution and are relatively inexpensive, making them suitable for real life applications [5]. Motor Imagery BCI (MI - BCI) is one of the EEG-based BCI that has been most researched from a vast number of possible applications. Users can envision performing specific movements, such as hand or tongue movement, which activates the sensorimotor cortex even without performing an actual motor movement. This cognitive simulation produces a brain reaction called Event-Related Desynchronization (ERD). ERD is defined as a decrease in the amplitude of mu (8-12 Hz) and beta (13-30 Hz) oscillations over sensorimotor areas during a motor imagery task. For MI based BCI classification systems to work, the appearance of ERD is necessary; it is an interpretable and reliable neural marker for differentiating between various imagined actions [6, 7].

Significant attention and effort have been directed on MI-BCI over the past few years to improve MI-BCI using innovative feature extractions and classification strategies. Feature extraction is necessary to identify significant patterns in EEG data that are most useful for detecting important information associated with motor imagery to more efficiently classify motor imagery

actions. The most commonly employed techniques were CSP (Common Spatial Pattern) and PSD (Power Spectral Density). CSP looks at spatial components by maximizing the differences in the variance of the tasks/classes. PSD looks solely at data in the frequency domain [8-10]. Oikonomou, et al. [8] investigated both CSP and PSD-based features for binary motor imagery classification using the Graz dataset B. It was found that PSD features were more effective combined with Support Vector Machine (SVM) than the CSP based approaches. The strongest results, with 79.33 % mean accuracy, were for those features when spectral information was obtained using Welch's method. They only focused on binary classification, did not include multi- domain data, and did not assess all nonlinear properties (i.e., bispectrum), therefore the research is limited in terms of its applicability to more complicated multi-class MI-BCI problems.

A hybrid framework integrating bispectral, entropy, and CSP characteristics was proposed in Hou, et al. [11], in which the BCI Competition IV dataset 2a was employed to differentiate between four motor imagery tasks (left hand, right hand, feet, and tongue) using a tree-based feature selection strategy and an RBF-kernel SVM classifier. An average accuracy of 71.61 % with a kappa coefficient of 0.621 was reported, exceeding single-feature baselines such as CSP alone (69.56 %) and bispectrum alone (46.76 %). However, although the necessity of incorporating spatial, statistical, and nonlinear characteristics was highlighted, time–frequency elements such as wavelet transforms, which are essential for capturing nonstationary signal dynamics, were not considered.

Similarly, multiclass motor imagery classification was examined by Olivas-Padilla and Chacon-Murguia [12] using a hierarchical SVM (HSVM) combined with wavelet packet decomposition and CSP for feature extraction. The proposed dual- layer model, integrating One-Versus-One (OVO) and One-Versus-Rest (OVR) SVM strategies, achieved an average accuracy of 64.4 % ± 16.7 % on the same dataset. Nevertheless, while the hierarchical design improved decision filtering, the absence of nonlinear features limited its ability to effectively distinguish between classes.

In contrast, an MI-BCI system was developed by Holm and Puthusserypady [13] to control drones using five motor imagery conditions, including left hand, right hand, both feet, tongue, and rest, where a modified Filter Bank CSP (FBCSP) algorithm with an SVM classifier was employed. Although the proposed method outperformed the winner of the BCI Competition IV dataset 2a (four-class MI), achieving a highest average accuracy of 68.5 % compared to 67.8 %, the five-class experiment resulted in an average accuracy of only 41.8 %, which was insufficient for real-time drone control. Moreover, despite the use of frequency- specific filtering, nonlinear and time–frequency features such as wavelet or bispectrum analysis were not incorporated, thereby limiting classification performance.

On the other hand, a multi domain feature extraction framework for EEG recognition was introduced by Guan, et al. [14], which combined time domain (MVAR), time frequency (wavelet packet), and spatial domain (Riemannian geometry) recognition approaches. Kernel Principal Component Analysis (KPCA) was then used to map the extracted features into a higher dimensional space, i.e., to extract nonlinear and multi-domain properties, before classification using a Radius-Incorporated Multi-Kernel Extreme Learning Machine (RIO-MKELM). Using this method, they obtained classification accuracy of 95.49 per cent. Nevertheless, the high accuracy is compensated by the complexity of the preprocessing and the feature extraction processes, and the computational intensity of the RIO - MKELM classifier, making the method less adequate for real-time BCI applications. This research suggests a multi-domain feature extraction technique which possesses a high accuracy level as well as computational efficiency, which is able to overcome the limitations encountered in previous studies especially related to the four classes motor imagery tasks. The proposed method uses power spectral density, log-variance, common spatial patterns (CSP), wavelet transform and bispectrum to extract the spatial information, spectral information, time-frequency and non-linear information of EEG signals accurately. A One Versus One (OVO) support vector machine (SVM) is used to further boost the classification accuracy, to improve the class separability and reduce the sensitivity to class imbalance. The whole system was tested on the BCI Competition IV dataset 2a and showed the potential to achieve high accuracy and computational efficiency, making it suitable for realistic MI -BCI scenarios.

Although several studies used classification accuracy as the main metric to assess them, practical motor-imagery based brain- computer interface (BCI) systems require a more thorough validation. In particular, decoded EEG decisions need to have temporal stability and be reliably translated in continuous and interpretable control actions. Therefore, in addition to traditional offline performance evaluation metrics, this work also introduces system-level validation based on an independent evaluation data set. This validation framework is aimed to measure temporal prediction consistency, EEG-driven motor command generation, coordination control behaviour and system robustness during continuous operation.

The structure of the paper is as follows: Section 2 describes our proposed methods containing feature extraction techniques and OVO-SVM classification. Section 3 reports on the results and compares our proposed methods with other approaches to date. Section 4 offers our conclusions and the future research directions.

2. MATERIALS AND METHODS

In this work, we describe a complete framework for multi-class EEG based classification that combines both linear and non- linear feature extraction techniques using a state-of-the-art classification model. Our method consists of multiple processing stages: dataset, pre-processing, feature extraction using PSD, log-variance, CSP, wavelet transform, and bispectrum analysis, followed by classification using SVM. The entire framework is illustrated in Figure 1, which outlines the pipeline from EEG signal input to final classification output.

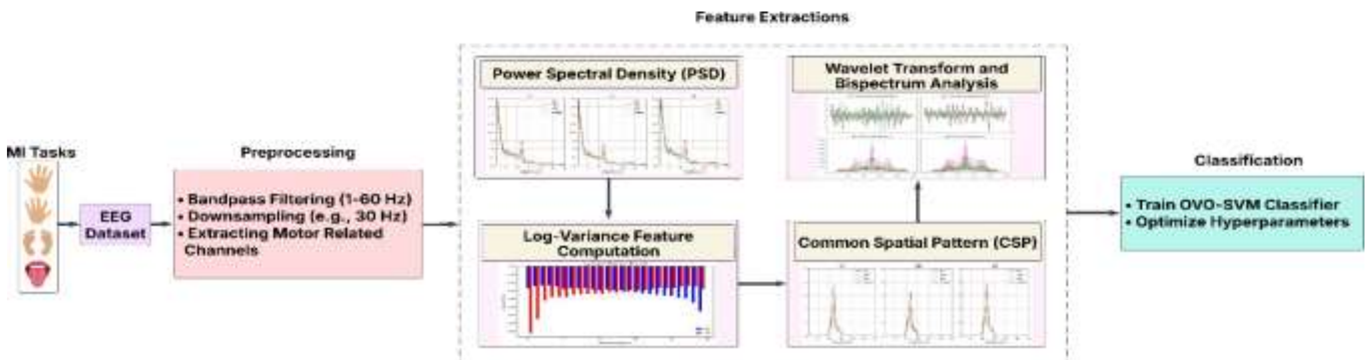

Figure 1. The proposed framework

2.1. Dataset and Preprocessing

The dataset used in this study is the BCI Competition IV dataset 2a, compiled by Graz University of Technology, Austria [15, 16]. This dataset contains EEG recorded from 9 subjects performing four modes of motor imagery tasks: left hand, right hand, both feet and tongue. The method of collection was a cue-based paradigm where subjects were cued to perform each motor imagery task while 22 Ag/AgCl electrodes recorded EEG signals. The EEG signals were sampled at 250 Hz; band-pass filtered from 0.5 Hz to 100 Hz. Each subject collected 2 sessions (1 training day and 1 testing day). Each session had 288 trials: this ensured a well-balanced dataset for all four classes.

Several preprocessing stages were performed in order to increase the quality of the data and extract the relevant features to prepare the EEG signals for the classification. First, the raw EEG signals were band pass filtered to eliminate noise from 1-60 Hz. This filter was effective in removing noise and the unhelpful components of frequency and preserving the primary oscillations in relation to motor imagery. Frequencies filtered specifically represent the alpha (8-12 Hz) and beta (13-30 Hz) bands, and the retained frequencies were deemed vital to the functioning of the motor imagery as these bands reflect activity associated with the motor cortex of the brain. After filtering, the EEG data were down sampled to 30 Hz in order to maintain important features while limiting the amount of information that the classification algorithm would have to process. For consistency in segmentation between trials and between subjects, data obtained between 0.5 and 2.5s after the task onset were discarded and the trials were segmented using event markers. The following channels were also selected from the EEG sensors: C3, Cz and C4, in order to augment the analysis since they are located over the motor cortex and related to motor-imagery classification, and thus represent enough brain activity.

2.2. Feature Extraction

Feature extraction represents an indispensable phase of motor imagery electroencephalographic classification since it attempts to transmute raw EEG signals into highly informative EEG signal representations that serve to augment class separability. In the current inquiry, a suite of complementary feature-extraction methodologies is implemented to represent the spectral, spatial, time-frequency and nonlinear characteristics that are inherent for EEG signals elicited during motor imagery tasks.

A. Power Spectral Density (PSD)

The Power Spectral Density (PSD) - the distribution of power of the signal in frequency regions - were computed for all channels at the first stage of the feature extraction. PSD allows to characterize modulation in the alpha (8-12 Hz) and beta (13- 30 Hz) frequency bands, known to be reliable indicators of motor imagery-related activity [17]. The estimation of PSD was done using the Fourier Transform, as outlined in Equation (1).

$$PSD(f) = |X(f)|^2 \tag{1}$$

Where, $X(f)$ is the Fourier Transform of the EEG signal $x(t)$. The considered frequency of interest was 1-30 Hz, this justified the consideration of alpha and beta bands associated with motor imagery. The PSD values calculated for all trials and each of the channels (C3, Cz, and C4) exhibited frequency specific energetic properties that provide the basis for identification of motor imagery events differentiating motor imagery tasks between actual motor tasks. The main input was features that were identified as relevant to perform subsequent processing and classification of these trials.

B. Log-Variance Feature Computation

Log-variance was calculated for each channel and trial to separate PSD features, highlighting relative power differences and stabilizing variance between trials. The log-variance for each feature component was calculated as defined in Equation (2), where $var(Z_h)$ denotes the variance of the h^{th} row of matrix Z.

C. Common Spatial Pattern (CSP) Transformation

The most significant aspect of our proposed feature extraction method is the use of Common Spatial Pattern (CSP) analysis to derive discriminative spatial features. CSP is designed to maximize the variance differences between two MI classes to improve discrimination between the two classes. The CSP algorithms use a projection matrix to project multichannel EEG signals into a lower-dimensional subspace [12, 18, 19]. The projection matrix (or spatial filter) is obtained through a simultaneous diagonalization of the covariance matrices of the two classes being discriminated. Given the EEG signal represented as matrix $E \in R^{N \times S}$, where N is the number of electrodes and S is the number of time samples, CSP computes a projection matrix W that transforms the signal into a new feature space, as expressed in Equation (3).

$$Z = WE \tag{3}$$

As a fact that CSP is inherently binary, we employ One-Versus-One approach to extend it to the four-class problem. In our work, separate CSP models are used to train each class pair (left vs. right, left vs. foot, left vs. tongue, right vs. foot, right vs. tongue, foot vs. tongue) to maximize the disparities between classes by creating spatial filters.

D. Wavelet Transform and Bispectrum Analysis

To enhance the linear spatial features derived from CSP, we utilize a nonlinear time-frequency analysis method that integrates Discrete Wavelet Transform (DWT) and bispectrum analysis on the most discriminative CSP components. This combination facilitates the extraction of both time-frequency and nonlinear features, which are crucial for identifying complex patterns in MI tasks [20, 21].

EEG signals are first decomposed into several frequency components at different temporal scales by using discrete wavelet transform (DWT). This decomposition is useful for identifying task-specific brain bands, in particular in the alpha band (8-12 Hz) and the beta band (13-30 Hz). The DWT of a signal $x(t)$ is formally defined as presented in Equation, (4).

$$W_x(a,b) = \int x(t)\psi^*\left(\frac{t-b}{a}\right)dt \tag{4}$$

Where, ψ is the mother wavelet, and a and b are the scaling and translation parameters, respectively. This transformation provides a time localized frequency representation of an electroencephalographic signal. Subsequent to extraction of the wavelet coefficients, bispectral analysis will be used to define nonlinear interactions and phase coupling in the signal. The bispectrum is defined as:

$$B(f_1, f_2) = E[X(f_1)X(f_2)X^*(f_1 + f_2)] \tag{5}$$

Where $X(f)$ is the Fourier Transform of the signal, and $X^*(f)$ is its complex conjugate. The bispectrum, as opposed to traditional spectral techniques, can measure higher-order statistical dependencies that can reflect smaller signal interactions that are necessary for distinguishing MI tasks. Our method enhances the discriminative power of the EEG representation used for classification by synthesizing wavelet and bi-spectral features.

2.3. Classification using SVM

After extracting spatial, spectral, and nonlinear features using CSP, PSD, and wavelet-bispectrum analyses, MI tasks are classified via the SVM algorithm. SVMs for EEG-BCI applications are widely utilized owing to their resilience to high dimensionality, non-linearly separable data, and generalizing power [22].

SVM finds the optimal decision boundary or hyperplane that separates classes as far apart as possible in the transformed feature space. To achieve this, kernel functions facilitate mapping the input features into a higher-dimensional space where linear separation is attainable [23]. Herein, we exploit an RBF kernel for an SVM classifier to exploit the complex relationships in the manifold that EEG features occupy. Because we conduct multi-class classification for four distinct MI tasks (left hand, right hand, foot, tongue), we implement an OVO approach. The OVO strategy builds a binary SVM classifier for every pairing of MI classes. This leads to a total of six classifiers in the OVO strategy. Each OVO classifier is trained for a specific pair of classes to capitalize when they are overlapped. This is done to maximize the classifiers' ability to cope with small inter-class differences, common challenges during MI classification using EEG activity. Hyperparameters, regulating the C regularization and the γ kernel coefficient, are tuned to improve SVM classifier performance. Tuning hyperparameters is crucial for optimizing generalizability performance, especially when the model is subject to multi-class EEG data where variability is often large.

The OVO-SVM classifier combined with common spatial pattern (CSP) for spatial filtering, power spectral density (PSD) for frequency-domain feature extraction and wavelet bispectrum analysis for time-frequency and nonlinear characteristics is a computationally efficient and robust methodology for the classification of motor-imagery (MI) electroencephalographic (EEG) signals. This way, the most discriminative features are ensured to be used and thus the classification accuracy is improved for multi-class MI tasks.

2.4. System Level Validation Using Evaluation Dataset and EEG Driven Motor Control

The current section outlines the system-level validation strategy taken here to test the proposed motor-imagery framework outside the boundaries of offline classification accuracy. An independent evaluation data is used to simulate the continuous EEG input, therefore allowing for an analysis of the temporal prediction stability and for the real-time conversion of the classification outputs into motor control commands. The validation framework focuses on the validation of the consistency of decoded motor- imagery decisions, reliability of motor-command generation and the adequacy of the proposed system for continuous EEG- driven control scenarios.

Practical motor-imagery brain-computer interface systems, aside from offline classification accuracy, have to be temporally stable, reliable in decision confidence, and have to be able to scale actuator response over long periods of operation. To meet these requirements, the proposed multiclass motor imagery framework is system-level validated on an independent evaluation dataset, and the goal is to validate the feasibility of the framework to convert EEG-based motor imagery intentions into continuous and interpretable motor control behaviour.

The overall operational flow of the proposed system is illustrated in Figure 2, which provides a complete visual overview from EEG data preparation to motor actuation. As shown in the diagram, the system begins with the training dataset used for the machine learning task. Raw EEG signals are first subjected to preprocessing, including band pass filtering, down sampling, artifact related signal refinement, and selection of relevant channels associated with motor cortex activity. Only the C3, Cz, and C4 channels are retained in order to reduce computational complexity while preserving discriminative motor imagery information.

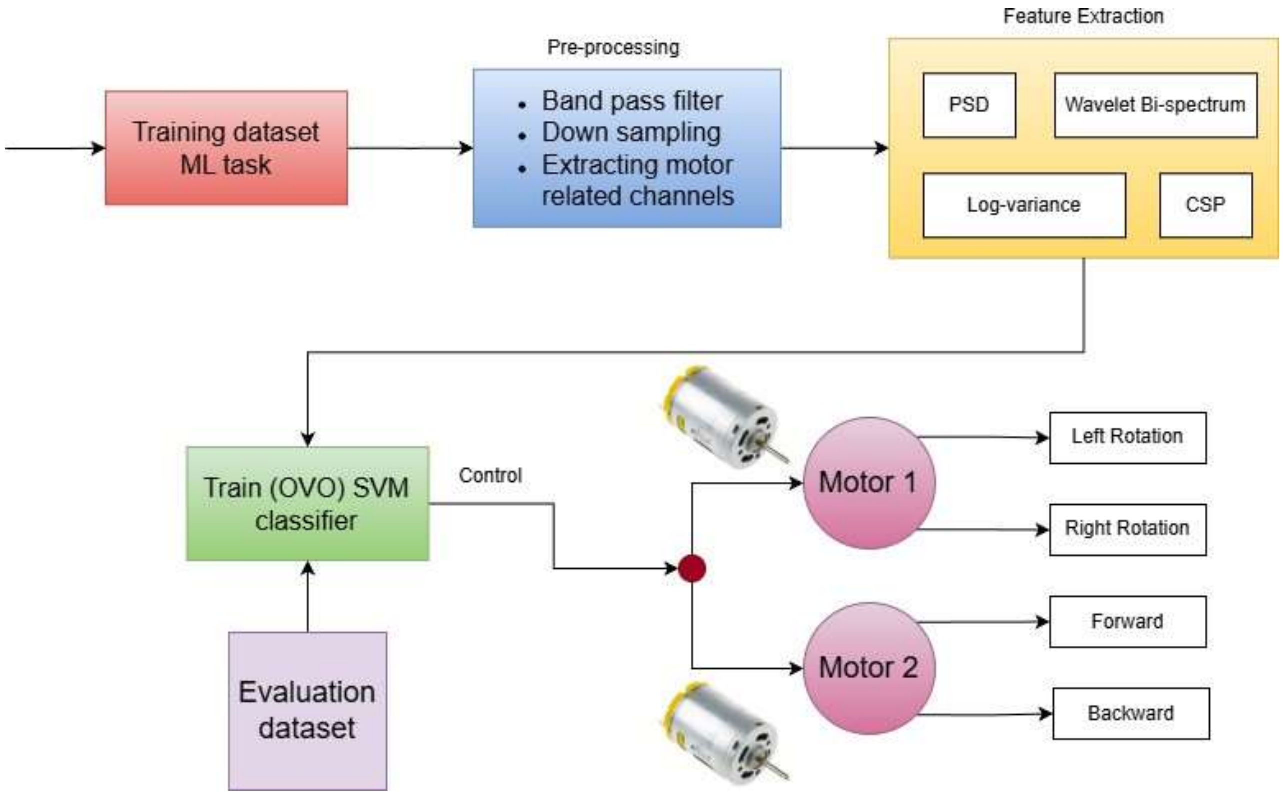

Figure 2. Block diagram of the proposed EEG driven motor imagery system

The proposed block diagram given in Figure 2 illustrates the complete signal flow of the EEG driven motor imagery control system, starting from dataset preparation and ending with actuator motion. The training dataset is first used to construct the machine learning model by applying preprocessing, feature extraction, and classifier training stages. During preprocessing, the raw EEG signals are filtered, down sampled, and reduced to the motor related channels in order to enhance signal quality and reduce computational complexity.

The preprocessed EEG segments are then passed to the multi domain feature extraction stage, where spectral features using power spectral density, statistical features using log variance, spatial features using common spatial pattern filtering, and time frequency and nonlinear features using wavelet and bispectrum analysis are extracted. These complementary features are provided to the one versus one support vector machine classifier, which is trained to discriminate among the four motor imagery classes.

During system operation, EEG data from the evaluation dataset follow the same preprocessing and feature extraction pipeline and are classified by the trained OVO SVM model. The classifier output represents the decoded motor imagery intention and is directly mapped to motor control commands through the control unit. Left hand and right hand motor imagery decisions generate left and right rotational commands for Motor 1, respectively, while tongue and foot motor imagery decisions generate forward and backward motion commands for Motor 2. This decision to action mapping enables the continuous conversion of EEG based motor imagery intentions into interpretable and coordinated motor control signals for two independent actuators.

3. RESULTS AND DISCUSSION

This section presents and discusses the experimental results obtained using the proposed multi-domain feature extraction and OVO-SVM classification framework. The performance of the system is evaluated through spectral, spatial, time-frequency, and nonlinear analyses, followed by quantitative classification assessment.

3.1. Spectral and spatial feature visualization

As is demonstrated in the Power Spectral Density (PSD) plots of raw EEG signals for the four MI classes in Figure 3, there are differences in strength for the four MI classes across the C3, Cz, and C4 channels. Of interest are the distinctions in the 10- 15 Hz band, which is in the alpha and lower beta bands, that will be associated with sensorimotor cortex activity for individuals executing imagined movements.

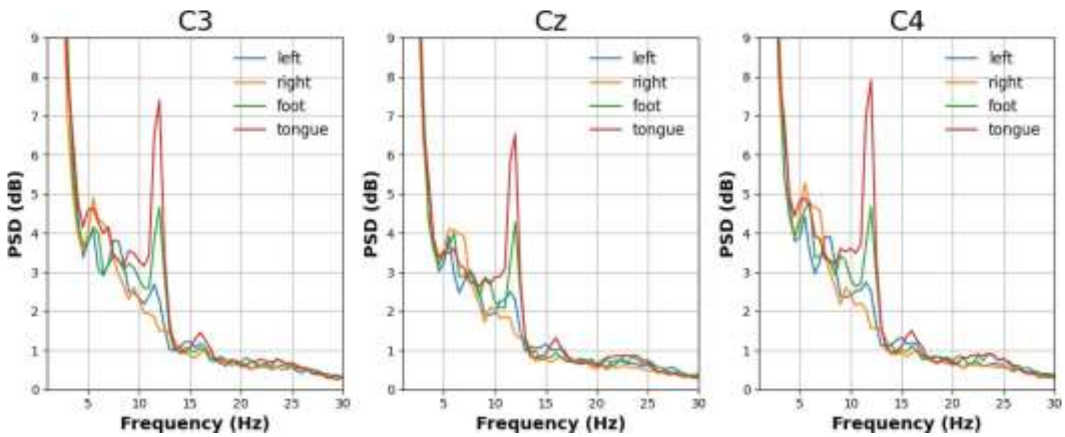

Figure 3. PSD of raw signals for four motor imagery tasks across channels C3, Cz, and C4.

Figure 3 shows that the motor-cortex activation in response to motor-imagery (MI) tasks is largely concentrated in the alpha and lower beta frequency bands (10 - 15 Hz). This observation confirms that these frequency ranges convey discriminative information relevant to MI activity and therefore justifies the use of a band-pass filter to isolate the relevant spectral components. Figure 4 shows the log variance features extracted across the recorded electroencephalographic (EEG) channels for each MI class, thus highlighting task related power distributions. The different variance profiles that were observed among the different classes showed how effective log variance features are at capturing relative power differences and for improving class discrimination.

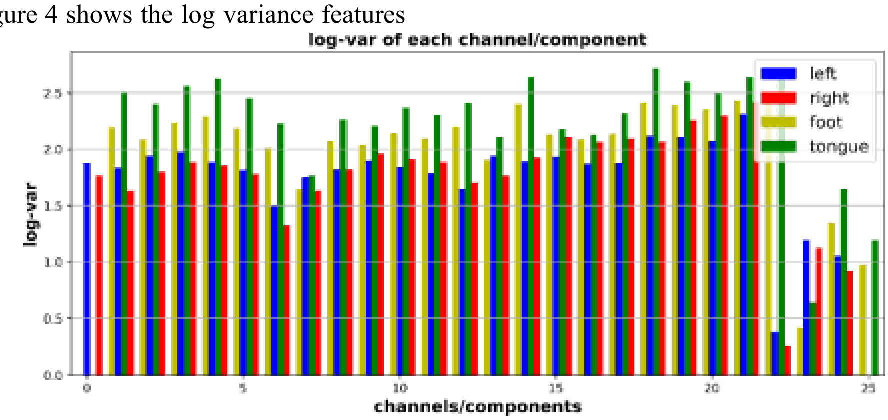

Figure 4. Log-variance values computed from the CSP components for each MI task.

To further enhance the class separability, the One vs. One Common Spatial Pattern (OVO-CSP) technique was used on all pairwise MI class combinations. Figure 5 shows an example of a spatial projection for the left vs. right hand motor imagery task, a representative CSP-based spatial projection, showing class-specific activation patterns and the ability of the OVO-CSP approach to differentiate between closely related MI classes.

.

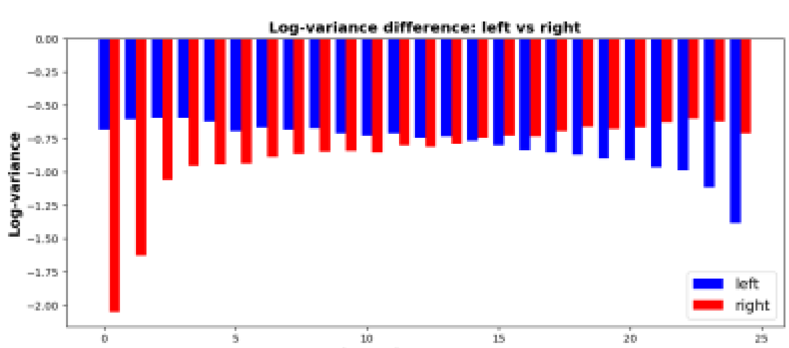

Figure 5. Log-variance differences for selected motor imagery class pairs (Left vs. Right) using the One-Versus-One CSP strategy.

To complement the separation of classes, the power spectral density was then computed for the components that resulted from common spatial pattern transformation. Figure 6 presents the PSD of first, median and the terminal spatial components where we can see an improved frequency separation, and more pronounced peaks, especially for the components with maximum variance. These findings suggest that CSP affects not only the spatial, but also spectral contrast between motor imagery tasks.

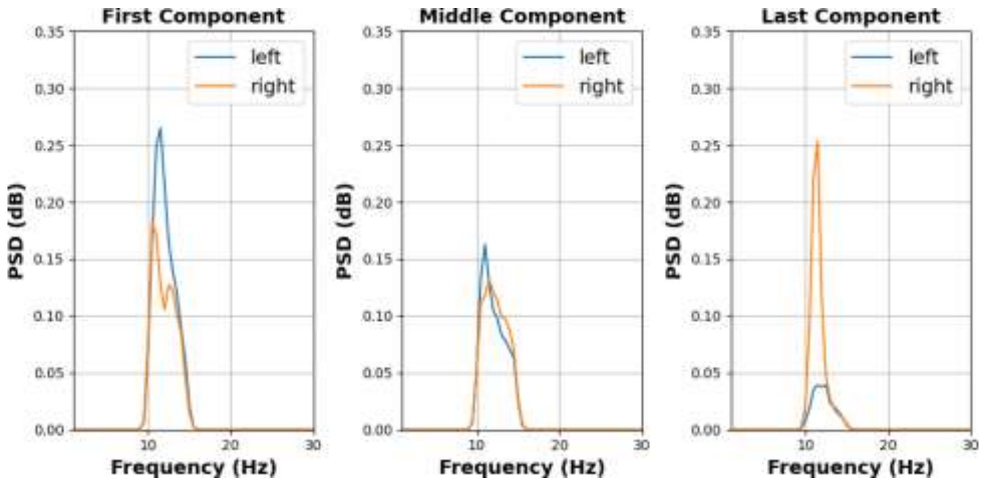

Figure 6. PSD of the first, middle, and last CSP components for the four MI classes. CSP filtering amplifies task-relevant frequency bands, enhancing discriminability in the spectral domain.

3.2. Time-Frequency and Nonlinear Feature Visualization

The first and last common spatial pattern (CSP) components resulting from the right-hand motor-imagery data set were investigated using wavelet transform and bispectrum analysis to shed some light on their temporal, spectral and nonlinear characteristics. Using Daubechies-4 (db4) wavelet and five levels of wavelet decomposition, the wavelet transform provides multiresolution representation enabling capturing of temporally localized signal dynamics relevant for motor-imagery cognition. Figure 7 shows that the first CSP component has an increased wavelet energy with prominent bispectral peaks, both indicating strong time-frequency activations and strong nonlinear phase coupling. Conversely, the terminal CSP part shows reduced and more erratic patterns, which suggests a relatively reduced role in discriminating motor imagery states.

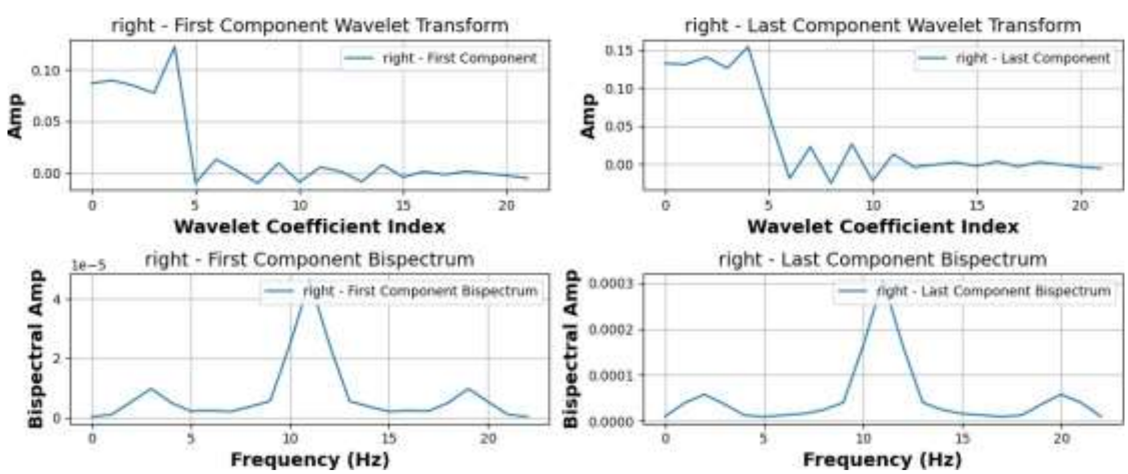

Figure 7. Wavelet and bispectrum analysis of right-hand motor imagery CSP components.

Figure 8 shows the wavelet and bispectral analyses of the first and the last common spatial pattern (CSP) components for the left hand motor imagery class. In a similar way to the right hand case, the first CSP component shows predominant energy concentrations of wavelets and also well-defined bispectral structures, suggesting meaningful nonlinear interactions and task- related temporal dynamics. On the other hand, the last CSP component exposes attenuated wavelet coefficients and less discernible bispectral features, which seems to be of limited relevance for effective motor imagery classification.

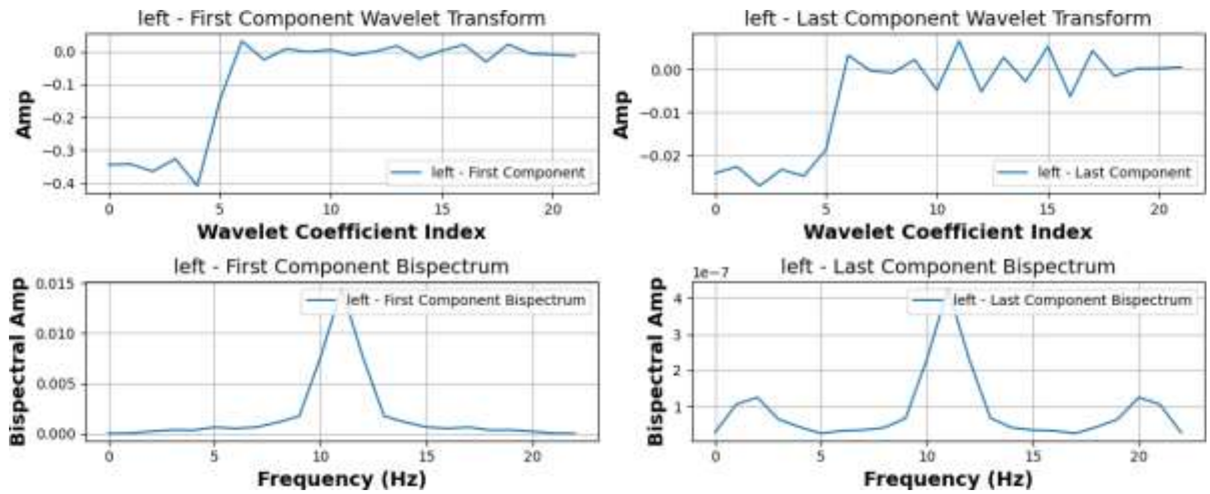

Figure 8. Wavelet and bispectrum analysis of left-hand motor imagery CSP components.

These results are consistent with findings of the power spectral density (PSD) analysis (see Figure 6), which contain spectral peaks in the mu (8-12 Hz) and beta (13-30 Hz) bands for the first common spatial pattern (CSP) components. Wavelet transforms complement this observation by revealing the temporal dynamics of the peaks while bispectrum analysis reveals nonlinear relationships between them. For the PSD plots showing clear peaks at certain frequency regions in the first versus the last CSP components, wavelet analysis helps to outline the temporal patterns or transients of those frequency regions. Collectively, these complementary methodologies provide a solid framework: PSD detects spectral content, wavelet analysis detects time localized transients, and bispectrum detects nonlinear couplings, which increases feature extraction for motor imagery based brain- computer interfaces. Accordingly, in Figure 9, a scatter plot is given to compare the bispectral features of the first and the last CSP components for the left- and transmembrane motor imagery classes. The different distributions indicate the differences in phase and amplitude dynamics, which strengthens the class separability and supports the effectiveness of nonlinear EEG features for the improvement of multi-class BCI classification.

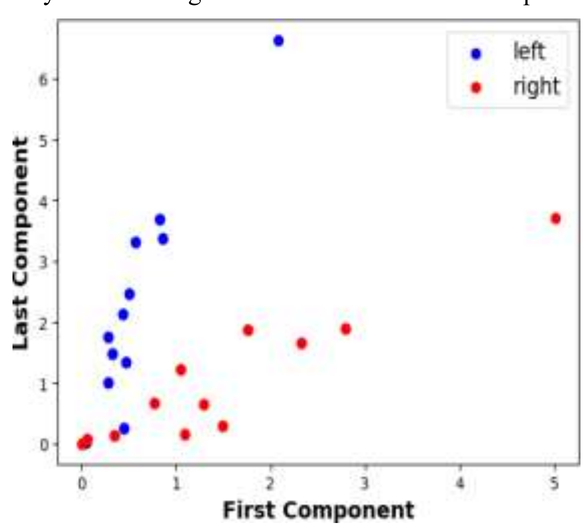

Figure 9. Bispectral feature scatter plot for left and right motor imagery (MI) task

3.3. SVM Classification

To evaluate the discriminative power of the CSP-transformed EEG features enriched by wavelet and bispectral analysis, an SVM classifier was employed to distinguish between motor imagery class pairs. The CSP projection matrix obtained after feature extraction was applied to both the training and test datasets to generate transformed components. As shown in Figure 9, the classification focused on the first and last CSP components due to their contrasting variance profiles and discriminative relevance. The SVM model was trained on the CSP-transformed features to distinguish between individual motor imagery class pairs (e.g., left- and right-hand motor imagery tasks), using an RBF kernel with tuned hyperparameters ($C = 1$ and $\gamma = 0.01$). The resulting classification boundaries are depicted in Figure 10, where the left subplot represents the training data and the right subplot shows the test data. Purple and yellow represent class 0 and class 1, respectively. The resulting decision boundary shows a high level of class separability for both of the datasets; moreover, the consistent separation found in the test data shows robust generalization and supports the discriminative power of the extracted csps-based features in combination with the optimized SVM classifier.

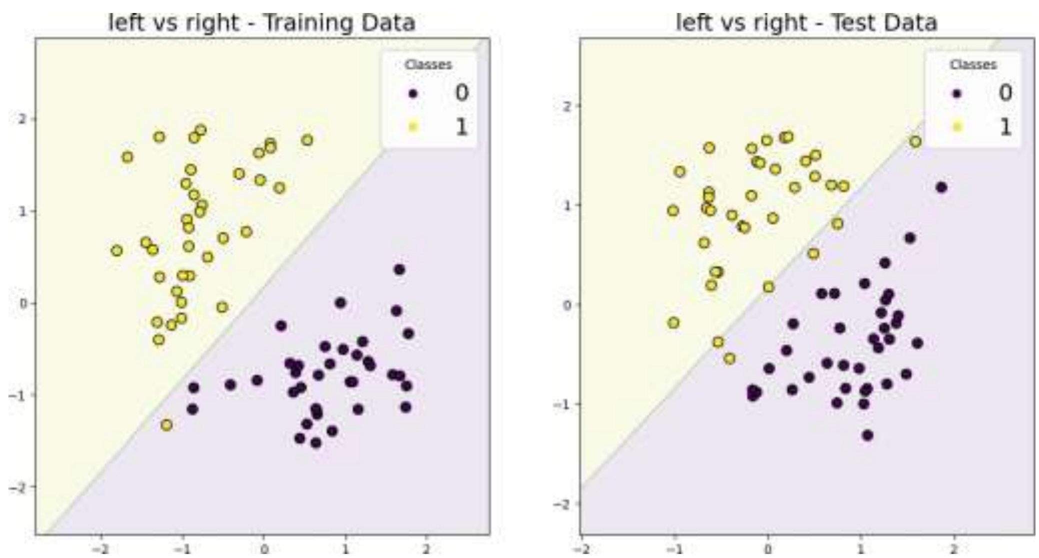

Figure 10. SVM classification boundaries in two-dimensional feature space.

3.4. Classification Performance and Evaluation

The confusion matrix related to the four motor imagery (MI) classes is shown in Figure 11. The classification accuracy of the proposed framework is high among all the categories with the left hand having a classification accuracy of 97 per cent, followed by the foot having a 96 per cent classification accuracy, the right hand with a 94 per cent classification accuracy and the tongue with a classification accuracy of 88 per cent. The overwhelming cause of misclassifications is between the tongue and foot, with 10 per cent of tongue trials being classified as foot.

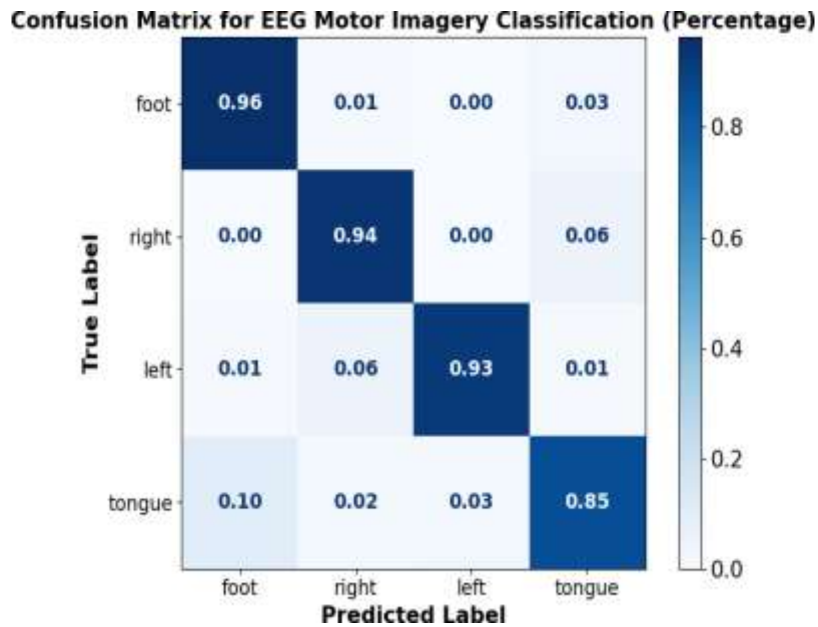

Figure 11. Confusion matrix showing classification accuracy for all MI class pairs.

Further information is given in Table 1, showing accuracy, precision, recall, and F1 - score for each motor imagery (MI) task pair. The right hand vs. foot classification resulted in the highest F1 - score (0.92) while the left hand vs. right hand classification resulted in the lowest (0.82). On average, the system achieved accuracy 88.05% precision 0.90 accuracy recall 0.87 and F1- score 0.89, which proved the consistency and reliability of discrimination on all class combinations.

Table 1: Classification metrics illustrating the impact of multi-feature fusion.

Class Pair	Accuracy (%)	Precision	Recall	F1-Score
Left Hand vs. Right Hand	76.39	0.85	0.79	0.82
Right Hand vs. Foot	97.22	0.93	0.91	0.92
Left Hand vs. Tongue	89.12	0.9	0.88	0.89
Foot vs. Tongue	91.47	0.92	0.9	0.91
Average	88.05	0.9	0.87	0.89

3.5. Subject-Wise Performance Evaluation

The proposed framework achieved an average accuracy of 74.3 per cent and kappa coefficient of 0.65, thus showing decent agreement and reliable generalization across all motor-imagery (MI) classes. When compared with preceding studies, it exceeded the performance reported by Hou, et al. [11] (accuracy of 71.61%) and it exceeded the kappa values reported in [24, 25]. Although Gómez-Morales, et al. [25] obtained a slightly higher accuracy (78.16%) with a kappa value of 0.56 which represented a weak inter class consistency and lack of generalization. Although some deep learning techniques, such as those proposed in [25], can lead to slightly better accuracies, they usually require large amounts of data and are very computation expensive. In contrast, the current machine learning framework optimizes the use of channels by using only three channels, thus reducing the computational and hardware requirements. On a per-subject basis, the system outperformed the benchmarks set by [11, 24] for most of the subjects, with Subject 3 showing the best results (95.83% accuracy, k=0.94). These subject specific classification results can be summarized in Table II highlighting the efficient tradeoff between performance and simplicity that make the proposed model a practical and deployable solution for real world MI-BCI applications.

Table 2: Comparison of subject-specific accuracy and kappa with previous studies [11, 24, 25].

Subject	Proposed Accuracy (%)	Proposed (K)	Accuracy in [11] (%)	(K) in [24] (%)	(K) in [25] (%)
1	87.96	0.84	80.9	0.63	0.31
2	60.19	0.47	64.24	0.17	0.53
3	95.83	0.94	85.76	0.88	0.67
4	64.81	0.53	65.63	0.38	0.89
5	66.9	0.56	44.79	0.69	0.24
6	53.01	0.37	54.17	0.41	0.34
7	65.74	0.54	84.38	0.76	0.63
8	87.27	0.83	84.03	0.76	0.8
9	87.04	0.83	80.56	0.69	0.6
Average	74.3	0.65	71.61	0.596	0.56

The following subsections go beyond an off-line classification assessment to consider system-level performance assessments. Using an independent evaluation data set the proposed framework is studied in continuous operation performing temporal prediction dynamics, decoded motor command generation, multi-motor coordination and resulting spatial motion patterns. This evaluation aims to verify that the proposed model achieves not only a high classification accuracy but also is stable and interpretable EEG-driven motor control in a realistic operational context.

3.6. Temporal Motor Imagery Prediction Analysis

According to the processes presented in section 2.4, multi domain feature extraction is performed by combining complementary feature types. Spectral characteristics are extracted using power spectral density, statistical power variations are captured using log variance, spatial discrimination is achieved through common spatial pattern filtering, and time frequency and nonlinear characteristics are obtained using wavelet and bispectrum analysis. These features jointly describe the spatial, spectral, temporal, and nonlinear properties of motor imagery EEG signals. The extracted features are then used to train a one versus one support vector machine classifier, which learns pairwise decision boundaries among the four motor imagery classes.

Once trained, the classifier processes EEG segments from the evaluation dataset in a fully automated manner without retraining. Each incoming EEG segment, corresponding to a 4 second decision window, is classified into one of four motor imagery classes, namely left hand, right hand, foot, or tongue. The classification output is directly mapped to motor control commands, where left hand and right hand imagery generate left and right rotational commands for Motor 1, while tongue and foot imagery generate forward and backward motion commands for Motor 2. This direct decision to action mapping enables continuous EEG driven motor control.

The trained model was evaluated using this operational framework on an independent evaluation dataset of 288 trials to give a cumulative continuous control duration of around 1,152 seconds. Figure 12 shows how the system predicts temporal variations in the prediction of motor imagery across the whole of the evaluation period. The results of the analysis show long periods of consistent prediction of classes, which means that the obtained multi-domain features can preserve the information related to the motor aspects in the EEG successive segments. Although short prediction transitions are seen they are very rare indicating the temporary ambiguity in the EEG signals and not the variability in the classifier.

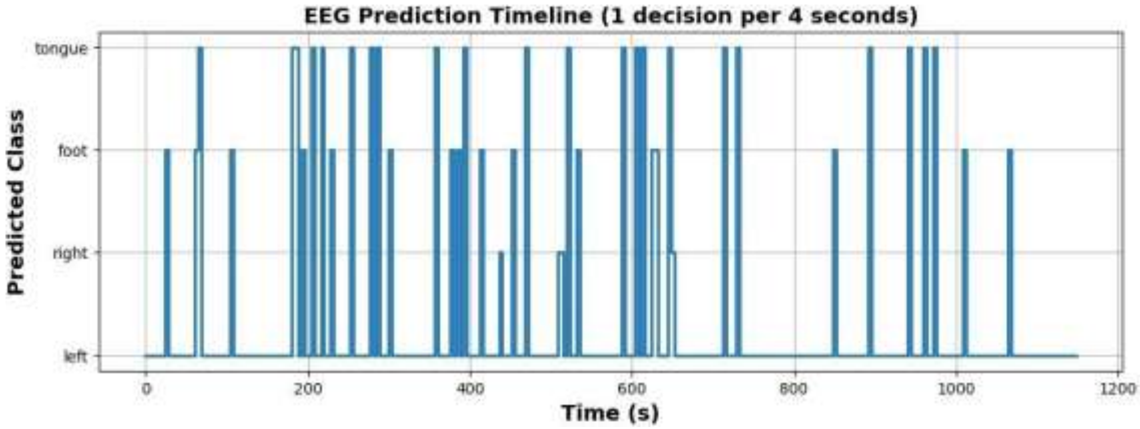

Figure 12. Temporal motor imagery prediction timeline over the evaluation dataset

To evaluate the consistency of the decisions, the voting behaviour of the one- vs-one support vehicle machine (SVM) classifier was studied. The average vote differentiation between the most likely class and the one that was second was 0.7465 which indicates a high degree of class separability and high confidence levels in the decisions made. There were also only 256 trials with low-confidence pattern, which is a vote margin of less than one. The correspondence between the vote-margin statistics and the reliably tight predictions intervals that are represented in Figure 12 offers further support to the strength of the classification stage.

3.7. Decoded Motor Command Generation and Actuator Stability Analysis

The motor commands based on the motor imagery choices made by the decision are shown in Figure 13, where the command signal of Motor 1 and Motor 2 are plotted as a function of time. Motor 1 performs left/right rotational controls based on the left- hand/right-hand motor images correspondingly, and Motor 2 controls forward/backward movements that are motivated by tongue/foot motor images. All the commands are produced at the same decision period of four seconds, thus providing uniform and systematic updates to the actuators during the span of the control. Long periods of steady-value command prove the consistency of actuators behaviour, which means that the rapid oscillation posing threats to the safety of the control is not observed.

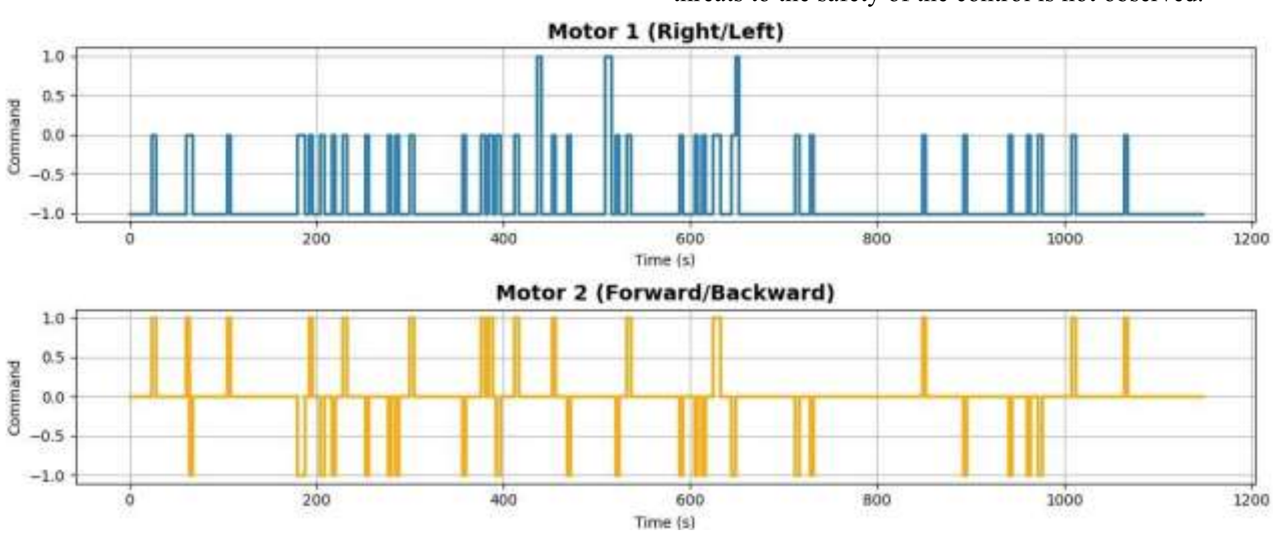

Figure 13. Motor command signals generated from decoded motor imagery decisions for Motor 1 and Motor 2 over time.

3.8. Coordinated Multi-Motor Command Execution Analysis

A detailed summary of the motor command signals is shown in Figure 14, and indicates the temporal traces of Motor

1 and Motor 2 on the same time frame. This description highlights the synchronised action of several motors and supports the fact that the actuators are complementary and do not contradict one another. The lack of competing commands proves the integrity of the class to actuator mapping and supports the credibility of the given control scheme.

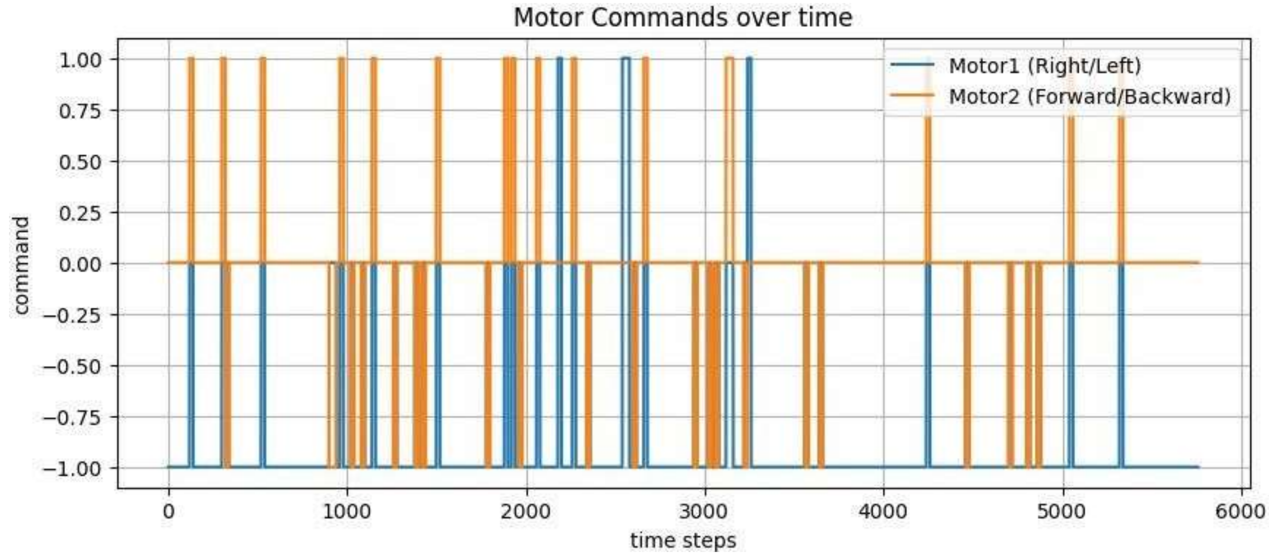

Figure 14. Combined motor command signals for coordinated multi motor control

3.9. Evaluation of Robot Path Continuity Using EEG Predictions

The space dynamics caused by EEG-motor commands are shown in Figure 15 that represents the two-dimensional trajectory of the robot within the whole period of evaluation. The trajectory represents the aggregate action of successive motor commands, representing coherent and progressive in place of stochastic or oscillatory motions. Minor deviations, which can be ascribed to the change of classes or low-confidence EEG segments detected during the previous analyses, are restricted and do not affect the continuity of an overall trajectory.

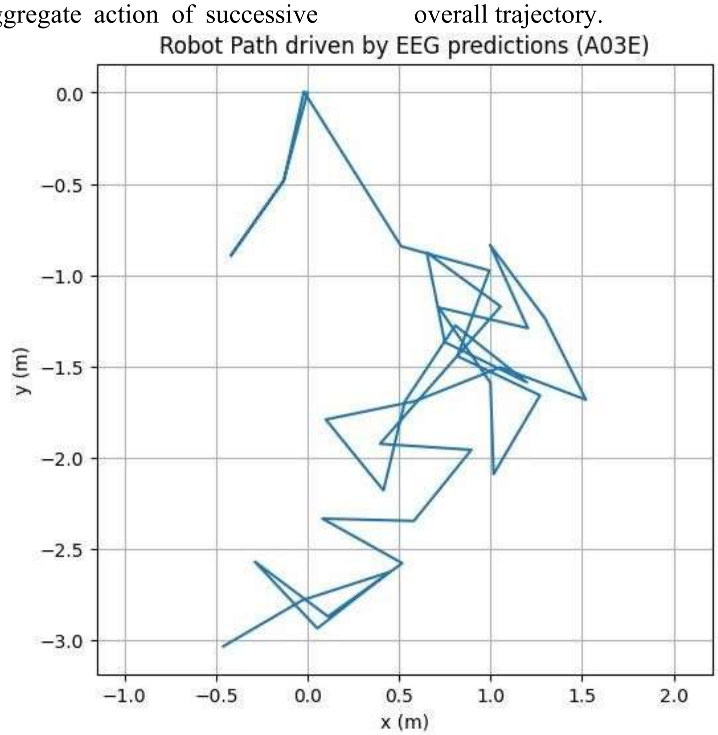

Figure 15. Two dimensional robot trajectory generated exclusively from EEG driven motor imagery control over the evaluation duration.

To provide a comprehensive understanding of the control mechanism illustrated in Figure 2, the complete generation and application of the motor command signals are described in detail. During system validation, the incoming EEG stream is segmented into consecutive temporal windows of 4 seconds, and each window is treated as an independent decision unit. For every EEG segment, the same preprocessing and multi domain feature extraction pipeline described in the methodology is applied, followed by classification using the trained one versus one support vector machine model. As a result, each EEG window produces exactly one motor imagery decision corresponding to one of the four classes: left hand, right hand, tongue, or foot.

The symbolic classification output is immediately converted into a numerical actuator command through a predefined decision to action mapping implemented in the control unit. This mapping is used to identify each motor-imagery class with a particular actuator and direction of motion so that the system can convert cognitive intentions to physical motion without any further post processing or smoothing. Control signals are updated after a fixed time interval of 4 seconds and any command stays constant within the entire decision window before the next EEG segment is processed.

Motor 1 is controlled by the first channel and it performs rotational movement. In case the decoded class relates to the left hand motor image, Motor 1 is given a command value of minus one, which means counter clockwise movement. When the decoded class is associated with right hand motor image, Motor 1 is given a command value of plus one, which refers to clockwise rotation. In case of tongue or foot images, Motor 1 is not activated or changed, because these categories are related to the translational movement controlled by the second actuator.

Motor 2 is controlled by the second control channel and serves as the motor of forward and backward motion. In the case where the decoded class is associated with tongue motor imagery, the command value to Motor 2 is a plus one which signifies forward movement. In case the decoded class is associated with foot motor imagery, Motor2 is given a command value of minus one meaning back movement. In the case of left or right imagery, Motor 2 is inactive or unchanged as it is only Motor 1 that takes care of rotational movement.

The control strategy produces two synchronised streams of commands which are discrete and interpretable motor actions, and the duration of each action is held to the duration of the associated EEG decision window. Long periods of steady command values show that motor-imagery decoding is consistent between sequential segments of EEG, but short periods between command values are associated with switching between visualised action or low-confidence EEG periods. The mechanism provides a smooth actuator behaviour and prevents high speed oscillations that may worsen the control performance.

The proposed framework can be used to provide continuous and robust EEG-based motor control by utilising multi-domain EEG feature extraction, one-versus-one SVM classification, and a direct decision to action mapping. The concordance in temporal prediction stability, consistency in actuator command, and consequent spatial movement observed indicates that the system is able to transform the motor-imagery intentions into coordinated physical motion which is the gap between offline EEG recognition and viable brain-computer interface control applications.

Lastly, the obtained results indicate that the multi-domain motor-imagery model attains stable temporal prediction behaviour, certain decision making, active multi-motor actuation and significant spatial motion. This top-level cheque upholds the fact that this approach is no longer only an offline EEG-based system but can be used to reliably convert motor-imagery intentions into readable motor-control commands, which is why this approach is relevant in the future to real-time brain-computer interface applications.

4. CONCLUSIONS

The current research proposed a multi-feature multi-class motor-imaging electroencephalographic (EEG) classification to combine spatial, spectral, time-frequency, and nonlinear features, which are obtained using the Common Spatial Patterns (CSP), Power Spectral Density (PSD), and wavelet transform, and bispectral analysis. Another support-vector machine, one-versus-one (OVO-SVM) classifier, was used further to enhance the discriminative ability of the system that the system was able to categorise accurately pairwise between motor-imagery tasks. Subject3 with a weighted Cohen 0.94 and an accuracy of 95.83 indicates the best level of classification, which proves the effectiveness of this system with subjects whose motor-imagery patterns are strong. Although there is inter- subject variability inherent, the general mean of 74.3% and 0.65 of kappa value indicate that they generally generalised the subject to subject.

In addition to achieving high offline performance and accuracy, the study offered detailed system-level validation of the proposed framework by an end to end EEG controlled motor-control system. The designed pipeline consists of pre-processing, multi-domain feature extraction, the use of an OV-SVM classifier, and a direct decision-to-action mapping tactic which transforms the decoded motor-imagery intentions into simultaneous control signals that drive two autonomous actuators. Long- run running with an independent assessment dataset is an affirmation of predictive stability in time, reliable judgement, consistent command execution, multi-motor behaviour and integrated spatial movement patterns.

The control mechanism of the devised can produce discrete motor actions at a constant frequency of decision and maintain them in consecutive EEG windows and produce smooth actuator dynamics and sound conversion of cognitive intentions in physical motion. These results prove that the offered strategy is effective in the context of the gap between EEG-based classification and the practical implementation of motor-control. The framework, therefore, has a high level of potentiality in real-life implementation of EEG-based control systems, such as autonomous systems and assistive robotics.

Despite the fact that the multi-class motor-imagery classification is still difficult because of the overlapping neural signatures and the inter-subject variation, the findings made support the validity and strength of the system in continuous control case. Future research will be aimed at confirming the framework in real-time brain-computer interface (BCI) uses and also determining its responsiveness, flexibility and usability in dynamic, user-interactive contexts.

References

1. M. del Carmen Malbrán, "World Report on Disability," *Journal of Policy & Practice in Intellectual Disabilities,* vol. 8, 2011.
2. S. K. Hadjidimitriou and L. J. Hadjileontiadis, "Toward an EEG-based recognition of music liking using time-frequency analysis," *IEEE Transactions on Biomedical Engineering,* vol. 59, pp. 3498-3510, 2012.
3. J. R. Wolpaw and D. J. McFarland, "Control of a two-dimensional movement signal by a noninvasive brain-computer interface in humans," *Proceedings of the national academy of sciences,* vol. 101, pp. 17849-17854, 2004.
4. C. H. Nguyen and P. Artemiadis, "EEG feature descriptors and discriminant analysis under Riemannian Manifold perspective," *Neurocomputing,* vol. 275, pp. 1871-1883, 2018.
5. G. Müller-Putz and S. C. Wriessnegger, "Electroencephalography and brain–computer interfaces," in *Neuroprosthetics and Brain-Computer Interfaces in Spinal Cord Injury: A Guide for Clinicians and End Users*, ed: Springer, 2021, pp. 71-103.
6. Y. Jeon, C. S. Nam, Y.-J. Kim, and M. C. Whang, "Event-related (De) synchronization (ERD/ERS) during motor imagery tasks: Implications for brain–computer interfaces," *International Journal of Industrial Ergonomics,* vol. 41, pp. 428-436, 2011.
7. G. Pfurtscheller and F. L. Da Silva, "Event-related EEG/MEG synchronization and desynchronization: basic principles," *Clinical neurophysiology,* vol. 110, pp. 1842-1857, 1999.
8. V. P. Oikonomou, K. Georgiadis, G. Liaros, S. Nikolopoulos, and I. Kompatsiaris, "A comparison study on EEG signal processing techniques using motor imagery EEG data," in *2017 IEEE 30th international symposium on computer-based medical systems (CBMS)*, 2017, pp. 781-786.
9. E. Dong, C. Li, L. Li, S. Du, A. N. Belkacem, and C. Chen, "Classification of multi-class motor imagery with a novel hierarchical SVM algorithm for brain–computer interfaces," *Medical & biological engineering & computing,* vol. 55, pp. 1809-1818, 2017.
10. S. Razi, M. R. K. Mollaei, and J. Ghasemi, "A novel method for classification of BCI multi-class motor imagery task based on Dempster–Shafer theory," *Information Sciences,* vol. 484, pp. 14-26, 2019.
11. Y. Hou, T. Chen, X. Lun, and F. Wang, "A novel method for classification of multi-class motor imagery tasks based on feature fusion," *Neuroscience Research,* vol. 176, pp. 40-48, 2022.
12. B. E. Olivas-Padilla and M. I. Chacon-Murguia, "Classification of multiple motor imagery using deep convolutional neural networks and spatial filters," *Applied Soft Computing,* vol. 75, pp. 461-472, 2019.
13. N. S. Holm and S. Puthusserypady, "An improved five class MI based BCI scheme for drone control using filter bank CSP," in *2019 7th International Winter Conference on Brain-Computer Interface (BCI)*, 2019, pp. 1-6.
14. S. Guan, T. Dong, and L.-k. Cong, "Method for EEG signal recognition based on multi-domain feature fusion and optimization of multi-kernel extreme learning machine," *Scientific Reports,* vol. 15, p. 6601, 2025.
15. C. Brunner, R. Leeb, G. Müller-Putz, A. Schlögl, and G. Pfurtscheller, "BCI Competition 2008–Graz data set A," *Institute for knowledge discovery (laboratory of brain-computer interfaces), Graz University of Technology,* vol. 16, p. 34, 2008.
16. *BCI Competition IV, "Datasets for BCI Competition IV," Brain-Computer Interface (BBCI). [Online]. Available: https://www.bbci.de/competition/iv/. [Accessed: Jan. 3, 2026].*

17. H. Göker, "Automatic detection of Parkinson's disease from power spectral density of electroencephalography (EEG) signals using deep learning model," *Physical and engineering sciences in medicine,* vol. 46, pp. 1163-1174, 2023.
18. S. Kumar, R. Sharma, A. Sharma, and T. Tsunoda, "Decimation filter with common spatial pattern and fishers discriminant analysis for motor imagery classification," in *2016 international joint conference on neural networks (IJCNN)*, 2016, pp. 2090-2095.
19. K. K. Ang, Z. Y. Chin, H. Zhang, and C. Guan, "Filter bank common spatial pattern (FBCSP) in brain-computer interface," in *2008 IEEE international joint conference on neural networks (IEEE world congress on computational intelligence)*, 2008, pp. 2390-2397.
20. B. A. Demirci, O. Demirci, and M. Engin, "Comparative analysis of ANN performance of four feature extraction methods used in the detection of epileptic seizures," *Computers in Biology and Medicine,* vol. 166, p. 107491, 2023.
21. B. Huang, G. Feng, X. Tang, J. X. Gu, G. Xu, R. Cattley*, et al.*, "A performance evaluation of two bispectrum analysis methods applied to electrical current signals for monitoring induction motor-driven systems," *Energies,* vol. 12, p. 1438, 2019.
22. V. D. Majety, N. Sharmili, C. R. Pattanaik, E. L. Lydia, S. R. Zeebaree, S. N. Mahmood*, et al.*, "Ensemble of Handcrafted and Deep Learning Model for Histopathological Image Classification," *Computers, Materials & Continua,* vol. 73, 2022.
23. K. Qi and H. Yang, "LS-GNHSVM: a novel joint geometrical nonparallel hyperplane support vector machine," *Expert Systems with Applications,* vol. 215, p. 119413, 2023.
24. J. Luo, X. Gao, X. Zhu, B. Wang, N. Lu, and J. Wang, "Motor imagery EEG classification based on ensemble support vector learning," *Computer methods and programs in biomedicine,* vol. 193, p. 105464, 2020.
25. Ó. W. Gómez-Morales, D. F. Collazos-Huertas, A. M. Álvarez-Meza, and C. G. Castellanos-Dominguez, "EEG Signal Prediction for Motor Imagery Classification in Brain–Computer Interfaces," *Sensors,* vol. 25, p. 2259, 2025.